Effect of electron-ion equilibration on optical emission from a shock wave

G. Chiu, A. Ng, and A. Forsman

Department of Physics and Astronomy, University of British Columbia, Vancouver, British Columbia, Canada V6T 1Z1

(Received 22 July 1997)

Optical emission from a shock wave emerging from a free surface is studied using numerical simulations taking into account the effect of temperature equilibration between electrons and ions. The results show significant variations depending on the equilibration rate. They also illustrate how measurements of the absolute intensity, relative spectral intensities, and temporal history of such emission can provide a new and important means for determining electron-ion equilibration rate in dense matter. [S1063-651X(97)50211-X]

PACS number(s): 52.35.Tc, 52.25.Fi, 52.25.Rv

Central to the study of high-density matter produced in a strong shock is the measurement of optical emission. For opaque materials, such observations are made on a free surface. The onset of optical emission signifies the arrival of the shock wave. This provides the usual means of measuring shock transit times and hence shock speeds. In the absence of preheat, the rate of increase in the intensity of emission at a planar free surface is governed only by the opacity of the unperturbed material and the shock speed [1,2]. For a metal, the emission rise time is typically of the order of picoseconds. Preheat of the material ahead of the shock front would be revealed by a much slower rise time [3]. The absolute and the spectral intensities of the emission form the basis for brightness and color temperature measurements, respectively [4]. Subsequent to shock breakout at the free surface, the rapid decay in the emission can be used to yield information on transport properties of the material in the rarefaction wave [5].

The analysis of optical emission from a shock wave has long been performed assuming equilibrium conditions. However, a recent experiment with silicon has suggested that substantial differences between the electron and ion temperatures exist in the region immediately behind the shock front [1,2]. The data also suggested a temperature equilibration rate two orders of magnitude slower than that predicted from the Spitzer-Brysk formalism [6]. In addition, recent molecular dynamics simulations with hot sodium ions and cold electrons have indicated a temperature relaxation time of nanoseconds [7]. For a proper interpretation of shock emission, the effects of temperature equilibration need to be included. Conversely, shock emission may provide an excellent means for studying energy exchange between electrons and ions in a strongly coupled plasma. In this letter, we will examine how various aspects of optical emissions can be used to assess the temperature equilibration rate between ions and electrons behind a shock front. The numerical study will focus specifically on opaque materials such as a metal to allow the consideration of a much broader class of materials other than silicon. The calculations will use a laser-generated shock wave as an example since they offer the only laboratory means for studying shock waves exceeding 10 Mbar (1 TPa). However, the findings should apply to shock waves produced by any other means. Our results will illustrate how the rate of temperature equilibration between electrons and ions affects the brightness, spectral intensity distribution, and temporal history of optical emission from a shock wave. This offers a possibility for probing electron-ion coupling in strongly coupled plasmas produced by shock compression of a metal.

The laser-driven shock wave and its optical emission are modeled using a one-dimensional, Lagrangian, hydrodynamic code [8] coupled with an electromagnetic wave solver. Details of the application of this code to the study of shock emission have been described elsewhere [2]. The shock state is treated as a two-temperature electron and ion fluid. A two-temperature quotidian equation of state [9] is used. The rate of energy exchange between the two species is assumed to be proportional to the mass density, the temperature difference, and a coupling coefficient, which is a free constant parameter except in regions of the expanding plasma where it exceeds the Brysk value [6]. In such regions, the local value of the Brysk coupling coefficient is used. The energy equations for the electrons and ions are given by

$$\frac{\partial}{\partial t}(\rho E_e) = -\frac{\partial}{\partial x}\left[\rho u\left(E_e + \frac{P_e}{\rho}\right)\right] + \frac{\partial}{\partial x}\left(\kappa \frac{\partial T_e}{\partial x}\right) + u\frac{\partial P_e}{\partial x} + \frac{\partial \epsilon_L}{\partial t} - g(T_e - T_i)\frac{\rho}{\rho_0}, \tag{1}$$

$$\frac{\partial}{\partial t}\left(\rho E_i + \frac{\rho u^2}{2}\right) = -\frac{\partial}{\partial x}\left[\rho u\left(E_i + \frac{P_i}{\rho}\right)\right] - \frac{\partial}{\partial x}\left[\rho u\left(\frac{u^2}{2}\right)\right] - u\frac{\partial P_e}{\partial x} + g(T_e - T_i)\frac{\rho}{\rho_0}, \tag{2}$$

where ρ is the mass density, u the fluid velocity, E the internal energy, P the pressure, κ the thermal conductivity, g the electron-ion coupling constant, ϵ_L the absorbed laser energy, and ρ_0 the normal mass density. Electron thermal conduction is treated using a harmonic-mean flux limiter model [10]. A flux limiter of 0.03 is used that takes into account flux saturation in the laser-driven ablation process. However, at the shock front the diffusive heat flux does not exceed the free-streaming flux.

To produce a sample 10-Mbar shock wave, we consider a temporally square laser pulse [full width at half maximum (FWHM) of 500 ps with rise and fall times of 150 ps] incident normally from vacuum onto a 10-μm-thick aluminum slab at an irradiance of 9×10^{13} W/cm^2. Aluminum is used as the sample material because of the availability of a wide range of data and models on its physical properties. The aluminum thickness is chosen to yield a steady shock wave

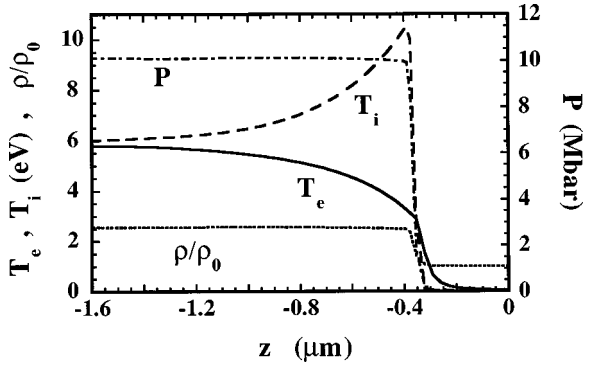

FIG. 1. Snapshots of pressure and temperature profiles of a 10-Mbar shock wave in-flight in aluminum. The free surface is at $z=0$.

at its rear surface in accordance with the laser pulse shape and duration. The temporally square pulse is an example of the Nova laser [11]. The short risetime of the pulse leads to a more rapid formation of a steady shock. Figure 1 illustrates the two-temperature structures of the resulting quasisteady shock at 2 ps prior to its arrival at the target free surface. The heating in front of the shock is due to electron thermal conduction. For an electron-ion coupling constant 10^{17} W/m^3 K, complete equilibration to the Hugoniot temperature occurs about 2 μm behind the shock front.

To calculate the intensity of optical emission from the shock wave as it approaches the free surface, an electromagnetic wave solver is applied as a postprocessor that solves the Helmholtz equations for a monochromatic electromagnetic wave entering the free surface from the vacuum. The optical properties of aluminum are derived from its complex dielectric function. This is formally equivalent to an atomic opacity model accounting for interactions with free electrons [12]. By applying an electromagnetic wave solver and Kirchoff's law, a spatial profile of emission at a specific wavelength is obtained. Figures 2(a)–2(c) show the emission profiles at different times. Prior to shock breakout, the extent of the emitting region is dominated by the opacity of the overdense material at the shock front. After the shock release, the emission is localized to the critical density layers of increasingly lower temperatures. To obtain the observed intensity, the spatial emission profile is integrated along the line of sight. The same procedure is repeated at successive times to yield the entire emission history. For comparison with experiment, the emission intensity is convoluted with the temporal resolution of the detectors. A similar method has been used to model optical emission from hot expanded states with equal electron and ion temperatures [5].

Figure 3 shows the calculated optical emission assuming various values for the electron-ion coupling constant g. The 2-ps convolution times represent a reasonable combination of temporal resolution and dynamic range of streak camera measurements. As g decreases, the peak emission intensity is reduced as a result of the lower electron temperature at the shock front. An even more drastic effect of the coupling constant is the temporal shape of the emission pulse.

In addition to electron-ion coupling the calculation of optical emission also depends on the electrical conductivity that governs the dielectric properties of the material. The results in Figs. 1–3 are based on electrical conductivities derived

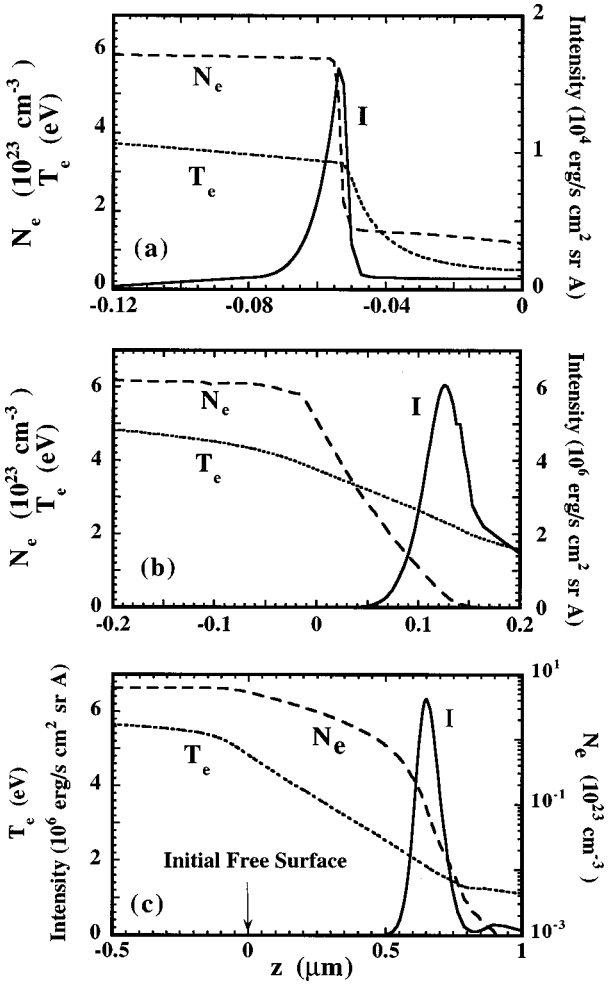

FIG. 2. Snapshots of density, temperature and 400-nm emission profiles: (a) 2 ps prior to shock arrival at free surface at $z=0$; (b) 5 ps after shock breakout; and (c) 22 ps after shock breakout.

from the Boltzmann transport model of Lee and More [13]. The only alternative conductivity model which corroborates experiments [14] and offers data over a sufficiently wide range of densities and temperatures is the density-functional-theory calculation of Perrot and Dharma-wardana [15]. In this model, however, the two-temperature treatment is limited to that with an ion temperature fixed at the lattice melting point. Figure 4 shows a comparison of the emission intensities calculated from the two conductivity models. The

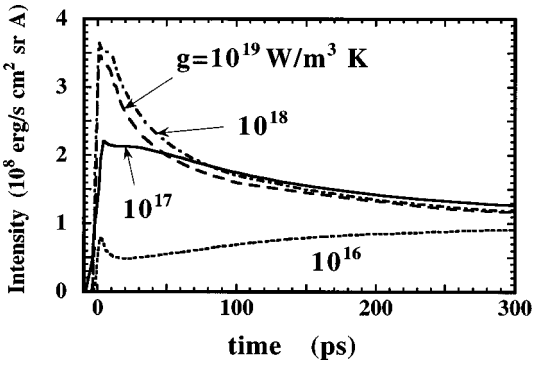

FIG. 3. Temporal histories of optical emission at 400 nm from a 10-Mbar shock wave in aluminum.

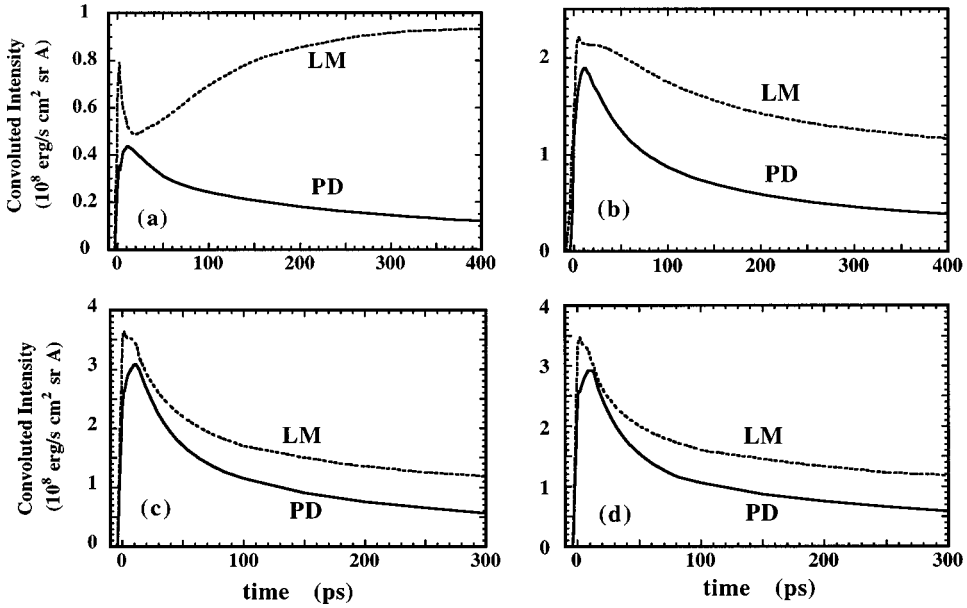

FIG. 4. Comparisons of 400-nm emission for Lee and More (LM) conductivity and Perrot and Dharma-wardana conductivity (PD): (a) $g=10^{16}$ W/m^3 K; (b) $g=10^{17}$ W/m^3 K; (c) $g=10^{18}$ W/m^3 K; and (d) $g=10^{19}$ W/m^3 K.

intensity and temporal variation of the emission are clear signatures of the electron-ion coupling constant and electrical conductivity of the shock-produced plasma.

To elucidate how the observed optical emission from a shock wave can be utilized, we consider experiments where the shock pressure is already determined either theoretically or experimentally. The former may be predictions from hydrodynamic simulations and the latter may involve the measurement of the shock speed. If only the absolute intensity of shock emission is measured, the data can be compared with theoretical predictions similar to those shown in Fig. 5 for the appropriate shock pressure. We have limited our consideration of the coupling constant between 10^{16} and 10^{19} W/m^3 K, following the findings of previous studies [1,2,16–20]. The difference in the absolute intensity for the two conductivity models is relatively small because, near solid density, both models yield similar conductivity values. Since absolute intensity calibrations can be made with accuracies of better than 10%, measurements of the absolute intensity of optical emission alone can readily provide a reasonable assessment of the electron-ion coupling constant.

If the reflectance of the shock wave is also measured, it can be used to determine the absorbance of the shocked material. Coupled with the measured absolute emission intensity this yields a brightness temperature directly via Kirchoff's law independent of electrical conductivity. The peak brightness temperature thus obtained can be compared with theoretical predictions shown in Fig. 6. Similarly, in experiments whereby the relative intensities of optical emission at different wavelengths and the corresponding reflectance are measured, the data can be used to yield a spectral temperature. Both of these offer another means of assessing the electron-ion coupling constant. The effect of finite temporal resolution of the experiment can be seen from the calculated brightness or spectral temperatures without the 2-ps convolution (Fig. 6). In this case, the calculated temperatures correspond to the electron temperatures at the shock front [Fig. 2(a)]. These are governed predominantly by the electron-ion coupling constant with a relatively weak dependence on the conductivity model through the effect of thermal conduction.

We have already pointed out that thermal equilibration between electrons and ions has a significant effect on the temporal characteristics of the optical emission (Figs. 3 and 4). At early times after shock breakout, the opacity of the released material is low, allowing regions with increasingly higher electron temperatures to be exposed. This leads to a

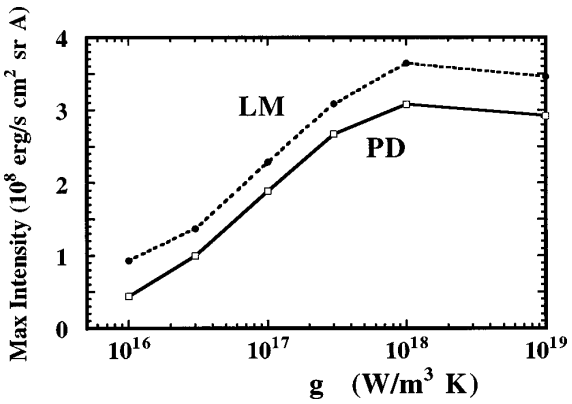

FIG. 5. Absolute intensity of emission at 400 nm from a 10-Mbar shock wave in aluminum calculated using LM conductivity and PD conductivity.

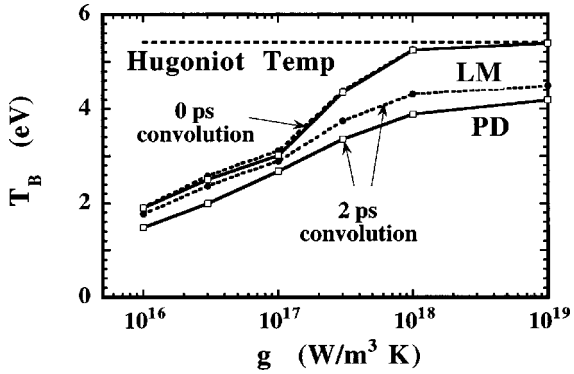

FIG. 6. Brightness temperature (T_b) and spectral temperature (T_s) as a function of g for Lee and More conductivity (LM: dotted lines) and Perrot and Dharma-wardana conductivity (PD: solid lines).

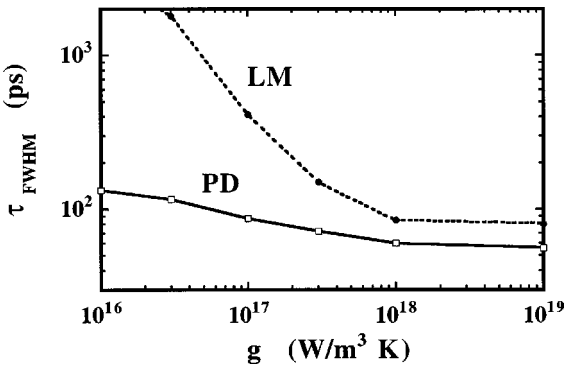

FIG. 7. The FWHM of the 400-nm emission pulse as a function of g for LM conductivity and PD conductivity.

continual increase in emission intensity and hence an increase in the rise time of the emission signal. However, very rapidly the opacity of the released material begins to dominate and the emission intensity starts to decrease. Nonetheless, thermal conduction mitigates the cooling of the released material, thus affecting the decay time of the optical emission. As the shocked material releases, the plasma electrical conductivity also plays an increasingly more important role as it determines the optical properties of the expanding plasma. The overall persistence of the optical emission can be characterized by its FWHM duration as presented in Fig. 7. These can serve as a sensitive measure of the electron-ion coupling constant for the Lee and More conductivity model. In any case, the detailed emission pulse shape will allow a definitive assessment of the coupling constant as evident from Figs. 3 and 4.

Our calculations have assumed the absence of preheat by suprathermal electrons [21] or x rays from the laser-heated plasma in the front side of the target. These are issues pertinent only to laser-driven shock waves. The suprathermal electron problem can be mitigated by keeping $I\lambda^2$ below 10^{14}, where I is the laser irradiance in W/cm^2 and λ the wavelength in μm. Even for 530 nm radiation, this allows an irradiance of up to 4×10^{14} W/cm^2 which yields a typical shock pressure of $\sim$30 Mbar. Radiative preheat can be mitigated using relatively thick targets or by generating the shock in a low-Z ablator such as CH before launching it into the aluminum sample. The latter also offers shock enhancement resulting from the impedance mismatch between CH and aluminum. Alternatively, the shock wave can be driven indirectly by converting the laser radiation into x rays [3]. Although a 10-Mbar shock wave is used here as an example, calculations for a shock wave of 30 Mbar yield similar features.

In conclusion, our results have illustrated the significant influence of electron-ion equilibration on the optical emission from a shock wave emerging at a free surface. We have also shown how the absolute intensity, brightness temperature, spectral temperature, the duration of emission and, in particular, its temporal history can all be used to assess electron-ion coupling in shock compressed matter. This approach does not require a semitransparent material, an inherent limitation of previously measurements on the electron-ion coupling constant [1,2].

We wish to thank R. M. More, Y. T. Lee, F. Perrot, and M. W. C. Dharma-wardana for the use of their theoretical models. This work was supported by the Natural Sciences and Engineering Research Council of Canada.

[1] P. Celliers, A. Ng, G. Xu, and A. Forsman, Phys. Rev. Lett. **68**, 2305 (1992).
[2] A. Ng, P. Celliers, G. Xu, and A. Forsman, Phys. Rev. E **52**, 4299 (1995).
[3] Th. Lower, R. Sigel, K. Eidman, I. B. Foldes, S. Huller, J. Massen, G. D. Tsakiris, S. Witkowski, W. Preuss, H. Nishmura, H. Shigara, Y. Kato, S. Nakai, and T. Endo, Phys. Rev. Lett. **72**, 3186 (1994).
[4] A. Ng, D. Parfeniuk, and L. Da Silva, Phys. Rev. Lett. **54**, 2604 (1985).
[5] P. Celliers and A. Ng, Phys. Rev. E **47**, 3547 (1993).
[6] H. Brysk, Plasma Phys. **16**, 927 (1974).
[7] U. Reimann and C. Toepffer, Laser Part. Beams **8**, 771 (1990).
[8] P. Celliers, Ph.D. thesis, University of British Columbia, 1987 (unpublished).
[9] R. M. More, K. H. Warren, D. A. Young, and G. B. Zimmerman, Phys. Fluids **31**, 3059 (1988).
[10] R. C. Malone, R. L. McCory, and R. L. Morse, Phys. Rev. Lett. **34**, 721 (1975).
[11] L. B. Da Silva, P. Celliers, G. W. Collins, K. S. Budil, N. C. Holmes, T. W. Barbee Jr., B. A. Hammel, J. D. Kilkenny, R. J. Wallace, M. Ross, R. Cauble, A. Ng, and G. Chiu, Phys. Rev. Lett. **78**, 483 (1997).
[12] R. Benattar, C. Galos, and P. Ney, J. Quant. Spectrosc. Radiat. Transf. **54**, 53 (1995).
[13] Y. T. Lee and R. M. More, Phys. Fluids **27**, 1273 (1984).
[14] A. Ng, P. Celliers, A. Forsman, R. M. More, Y. T. Lee, F. Perrot, M. W. C. Dharma-wardana, and G. A. Rinker, Phys. Rev. Lett. **72**, 3351 (1994).
[15] F. Perrot and M. W. C. Dharma-wardana, Phys. Rev. A **36**, 238 (1987).
[16] L. G. Fujimoto, J. M. Liu, E. P. Ippen, and N. Bloembergen, Phys. Rev. Lett. **53**, 1837 (1984).
[17] H. E. Elsayed-Ali, T. B. Norris, M. A. Pessot, and G. A. Mourou, Phys. Rev. Lett. **58**, 1212 (1987).
[18] R. W. Schoenlein, W. Z. Lin, J. G. Fujimoto, and G. L. Eesley, Phys. Rev. Lett. **58**, 1680 (1987).
[19] P. B. Corkum, F. Brunel, N. K. Sherman, and T. Srinivasan-Rao, Phys. Rev. Lett. **61**, 2886 (1988).
[20] R. H. M. Groeneveld, R. Sprik, and A. Lagendijk, Phys. Rev. Lett. **64**, 784 (1990).
[21] W. L. Kruer, *The Physics of Laser Plasma Interactions* (Addison-Wesley, Reading, MA, 1988) Chap. 13.